Fracture Mechanics of Concrete and Concrete Structures - Assessment, Durability, Monitoring and Retrofitting of Concrete Structures- B. H. Oh, et al. (eds)

Quantified estimation of rebar corrosion by means of acoustic emission technique

T. Shiotani
Kyoto University, Kyoto, Japan

M. Kunieda
Nagoya University, Nagoya, Japan

N. Okude
Tokai Technology Center, Nagoya, Japan

ABSTRACT: As for proactive maintenance for infrastructures, it is very important to assess the structural deterioration from the early stage. Rebar corrosion is one of the major damages in reinforced concrete structures and it is of high demand that corrosion levels can be estimated reasonably with nondestructive ways. In this study, flexural failure tests of RC beams having different weight loss of 0%, 5%, 10% and 30% were carried out with monitoring acoustic emissions, respectively. Attaching the sensors onto the concrete surface as well as rebar edge faces, AE activity were examined to extract characteristic AE features corresponding to the corrosion level. Through the experimental work, it was clarified that the number of AE events of high frequency dramatically decrease with progress of corrosion in comparison to those of low frequency when using the AE activity of rebar attached sensors. The ratio of AE events of low frequency to those of high frequency, which is defined as α-value, yields to provide the corrosion level quantitatively.

1 INTRODUCTION

Rebar corrosion is one of the severe deterioration in concrete structures, affecting safety of concrete structures. As accumulated corrosive damage within concrete structures was regarded to be not a trivial subject, past studies of this subject have been focusing to clarify the deterioration process due to corrosion i.e., dormant stage, initiation stage, accelerated stage and deterioration stage by nondestructive ways (Yoon et al. 2003, Ohtsu et al. 2003, Ohtsu & Tomoda 2008). Correspondingly there were few investigations on corroded RC members subjected to external loading with non-destructive testing. Indeed actual in-service RC structures like bridges are always subjected to flexural deformation due to mobile loads, namely transportation, it is very crucial to estimate the corrosion level in service condition. Thus in this study, for four different levels of corrosive RC, four-point bending was applied with monitoring AE. AE parametric features corresponding to the corrosion level are examined with different positioned AE sensors, namely on concrete surface and rebar edge face.

2 EXPERIMENT

2.1 *Specimen*

Specified mix proportions of concrete used in the tests are given as in Table 1. The cement, fine aggregate, and coarse aggregate were ordinary Portland cement with a density of 3.15 g/cm^3, river sand with a density of 2.55 g/cm^3, and river gravel (maximum size: 15mm) with a density of 2.57 g/cm^3, respectively. The chemical admixture was an air-entraining and water-reducing agent. The slump and air content of the mixed concrete were 7.5 cm and 2.2%, respectively. Beam specimens measuring 140 x 80 x 1460 mm were used for bending tests, as shown in Figure 1. A deformed rebar with a nominal diameter of 13 mm and nominal yielding strength of 345 MPa was placed in the specimen. All stirrups were wrapped with polyvinyl tape to prevent corrosion of stirrups themselves. One specimen was fabricated for each series. After being demolded at the age of 1 day, specimens were covered with wetting-cloth, and cured in a thermostatic room at 20°C for 28 days. Compressive strength of the concrete at the age of 28 days was 22.7 MPa.

2.2 *Accelerated corrosion tests and results*

In order to induce rebar corrosion, an accelerated corrosion tests were carried out for the beam as shown in Figure 2. The specimens were placed on a copper plate in a container filled with NaCl solution (concentration: 3%), and current of 0.6 A (0.907 mA/ mm^2) was applied to rebar in each specimen. Table 2 tabulates the investigated corrosion levels represented by different weight loss of rebar. The weight loss was controlled by total applied current. Here, the relationship between expected weight loss and total applied current has been proposed by Tamori et al. 1988. A good correlation between the weight loss and total applied current was observed in this test, as shown in Figures 3, 4 shows the longitudinal crack width measured at the bottom surface being close to the rebar. Basically, crack width became wider with increasing of the corrosion level represented by weight loss. In severe corrosion cases as more than 10%, crack width along a specimen axis was not constant, indicating that corrosion was not distributed uniformly along the rebar.

Figure 5 shows the diameter of rebar measured by a caliper with an interval of 50 mm. Nominal diameter of rebar used in this test was 13 mm. Remarkable decrease of rebar was locally observed especially in the case of most severe case of 30%.

Table 1. Mix proportions of concrete.

W/C	S/A	Unit content (kg/m^3)				
		W	C	S	G	Ad*
56.5	49.6	176	312	860	882	3.12

* AE water reducing agent

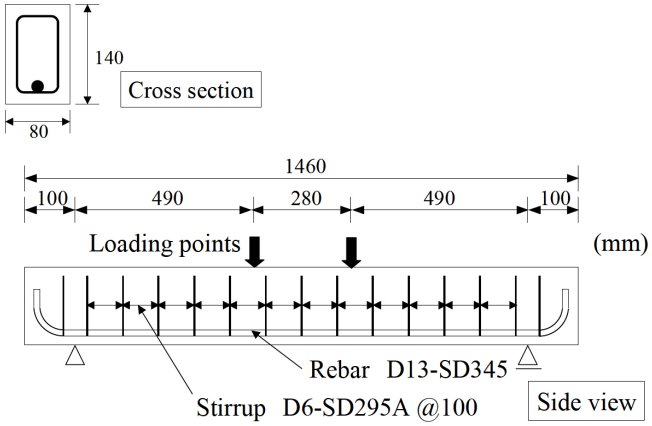

Figure 1. Configuration of tested specimen.

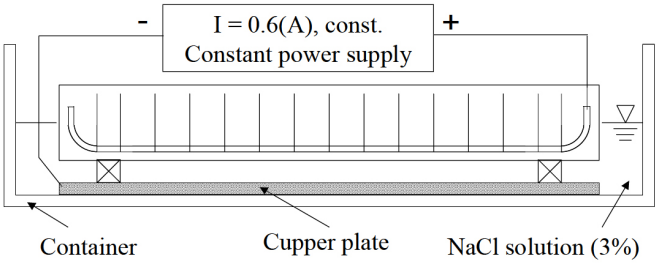

Figure 2. Overview of accelerated corrosion test.

Table 2. Weight loss of rebar after corrosion test.

	3%	10%	30%
Weight loss (%)	3.8	12.7	29.8
Total applied current (A/hr)	69.6	240	602.4

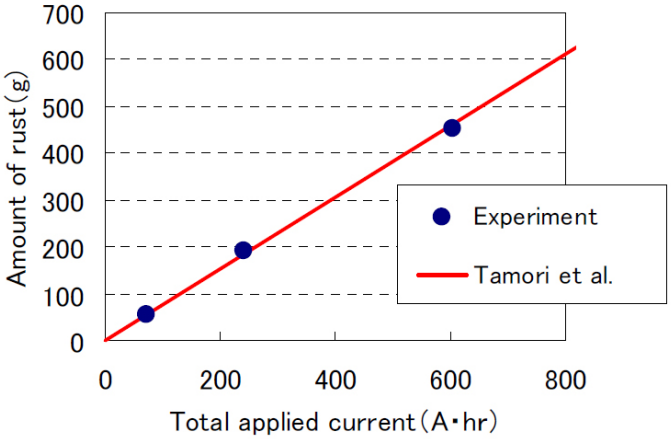

Figure 3. Amount of rust after corrosion test in comparison to the regression line obtained by Tamori et al.

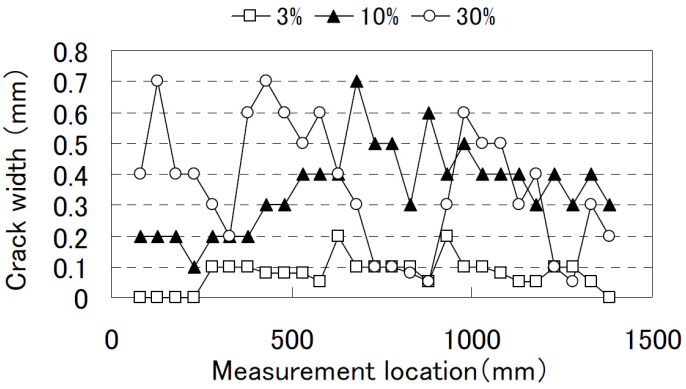

Figure 4. Crack widths along the bottom surface after corrosion test.

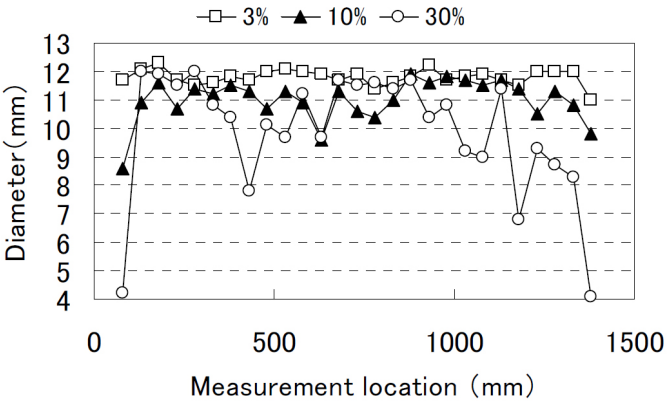

Figure 5. Measured diameters of rebar in a longitudinal direction after corrosion test.

2.3 *Loading tests and results*

Four-point bending tests were conducted with a constant moment length of 280 mm and total span of 1260 mm, as shown in Figure 1. During the test, load and displacement at loading points were also

measured by load-cell with a capacity of 100 kN (resolutions: 33 N) and LVDT with a capacity of 50 mm (sensitivity: 0.01 mm). Figure 6a shows measured load-displacement curves in all series. Globally, there was not significant difference between 0% case and 3% case. In other cases, however, yielding and maximum loads became lower with increasing of corrosion level (weight loss). Especially, in the case of 30%, rebar was finally broken. Figure 6b depicts the enlarged view of Figure 6a up to displacement of 5 mm, where unloading paths of each curve are removed. First cracking load of each case was similar to each other (see in Fig. 6b), but tension stiffening zones where debonding between rebar and concrete was taken place were slightly different. As shown in 30% case, corrosion of rebar gave less bond properties than others. Figure 7 represents the crack patterns after the loading tests. In the case of 0% with no corrosion, more than five cracks were observed, whereas quite small numbers of cracks, implying less bond strength in general, was observed in 30% case. In addition, the location of broken rebar agreed quite well with both locations showing wider crack width and minimum diameter of rebar, as found in Figures 4 and 5. As aforementioned during the flexural test, debonding between rebar and concrete was becoming dominant with progress of rebar corrosion.

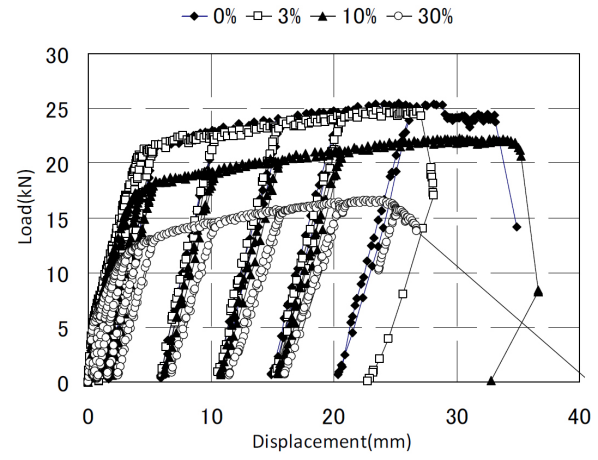

(a) Global behavior

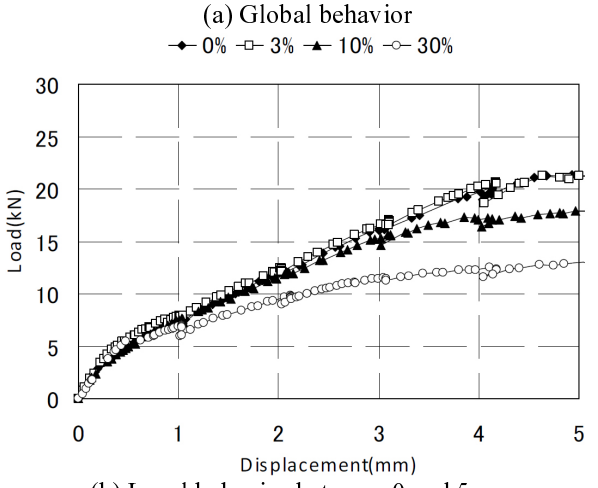

(b) Local behavior between 0 and 5 mm.

Figure 6. Load and displacement curves.

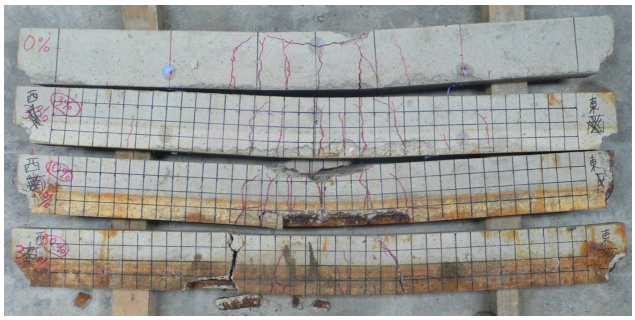

Figure 7. Photos of specimens after loading test. 0, 3, 10 and 30% from the top.

3 AE MEASUREMENT

3.1 *Monitoring condition*

AE sensors used for the monitoring were 150 kHz resonant of Vallen-systeme. AE signals detected by the sensor are amplified by 40 dB at preamplifier and the signals are further amplified by 40 dB at main-amplifier. The amplified signals exceeding the threshold level of 54 dB are recorded as their parametric features as well as waveforms by AMSY-5 (Vallen-systeme) AE monitoring equipment. Ten AE sensors were attached to the concrete surface; however, due to ambient noise AE data obtained only by four sensors are used for the further analysis. Besides two AE sensors were added to attach onto the rebar face as shown in Figure 8.

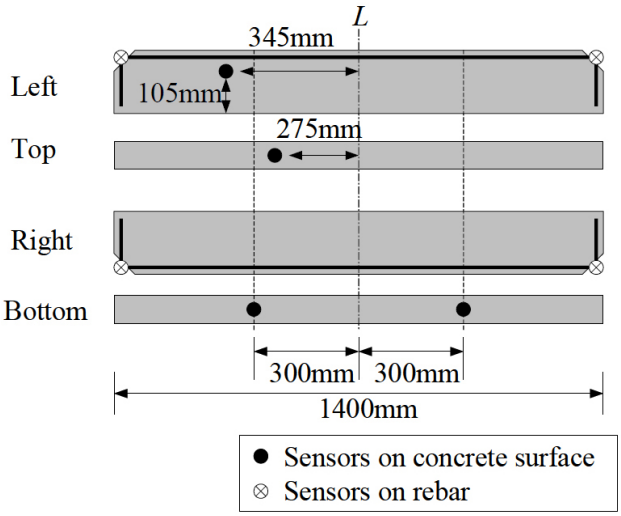

Figure 8. Arrangement of AE sensors.

3.2 *Results*

3.2.1 *AE activity*

AE hit rate with displacement can be found as in Figure 9, of which Figures 9a and b is one of concrete attached AE sensor and rebar attached AE sensor, respectively. As in Figure 9a, unique relations could not be obtained between AE activities and corrosion levels, whereas a common trend showing larger numbers of AE hits to 3-4 mm rather than those of 4-5 mm displacement can be confirmed. As the 4-

5 mm range corresponds to the region of rebar yield, this results in no further damage of concrete, leading to inactive behavior of AE in this range. Interesting AE activities with corrosion levels can be obtained from Figure 9b, which is of rebar attached AE sensor. AE activity becomes the highest in 30%, followed by that of 10%, 3% and 0% in turn. As for the number of AE hits in comparison to that of concrete attached AE sensor, extremely small numbers were obtained from the rebar. Two reasons are considered leading this fact: used sensor response around 150 kHz, which is relatively higher frequency than that used for large concrete, narrowing the detection areas so small limited around the rebar; and energy loss of elastic waves when they come into the rebar from concrete due to mismatch of acoustic impedance between concrete and rebar (Shiotani & Ohtsu 1999).

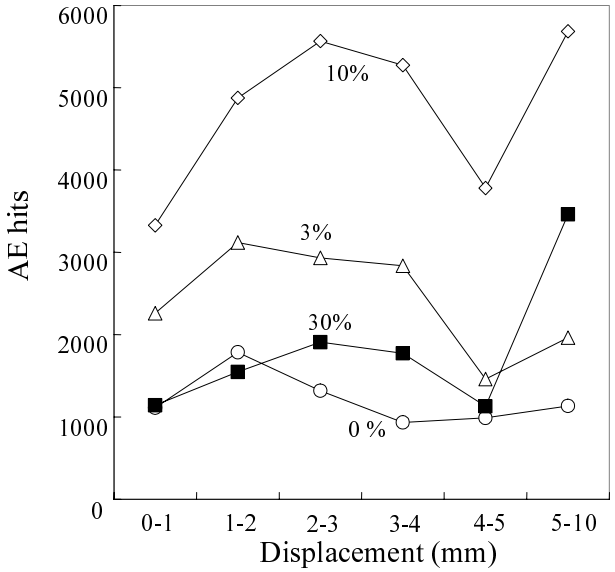

(a) Concrete attached AE sensor

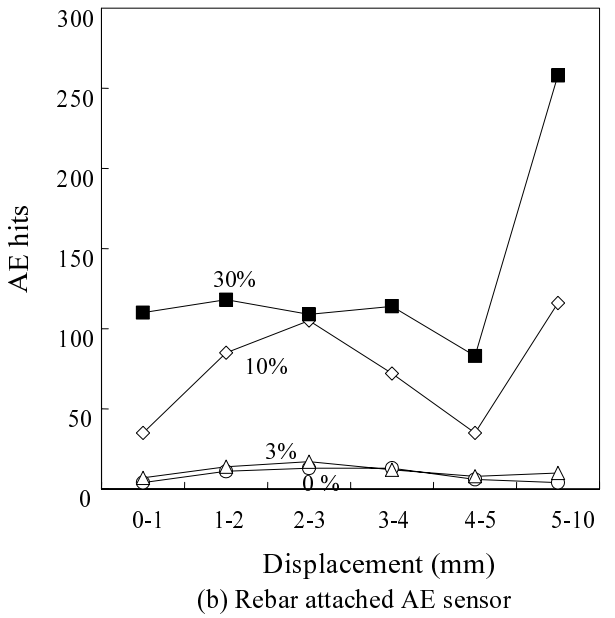

(b) Rebar attached AE sensor

Figure 9. AE hits rate with displacement.

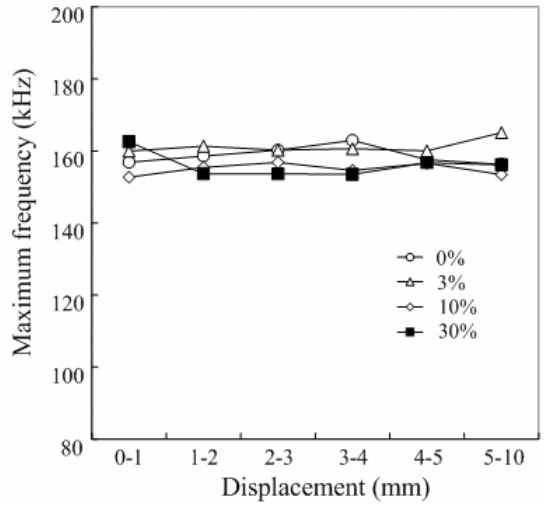

(a) Concrete attached AE sensor

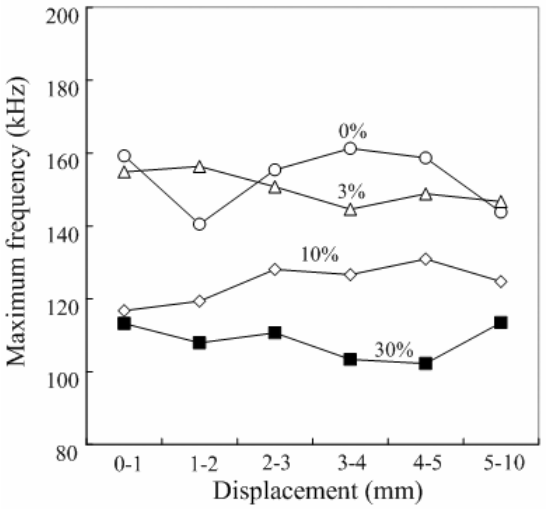

(b) Rebar attached AE sensor

Figure 10. Averaged max frequency with displacement.

3.2.2 *Frequency Analysis*

Averaged peak frequency with displacement can be found as in Figure 10, of which Figures 10a and b is one of concrete attached AE sensor and rebar attached AE sensor, respectively. The averaged peak frequency was obtained from averaging all of the derived peak frequencies through fast Fourier Transform (FFT) of recorded all the AE waveforms. Irrespective to the corrosion level, the peak amplitude appears a constant around 150 kHz that corresponds to the resonant frequency of AE sensors in the case of concrete attached one as found in Figure 10a. Decrease of peak amplitude with progress of corrosion level is obvious in case of rebar attached AE sensors as can be found in Figure 10b. It would be difficult to identify the specific cause leading the decrease corresponding to the corrosion level. Such reasons as crack patterns representing corrosion levels, and difference of restraining condition of rebar by surrounding concrete corresponding to the corrosion level, appeared to attribute to this fact.

Raw data of peak frequency through FFT are shown in Figure 11. Two extremely cases of 0% (in tact) and 30% of corrosion level are demonstrated as

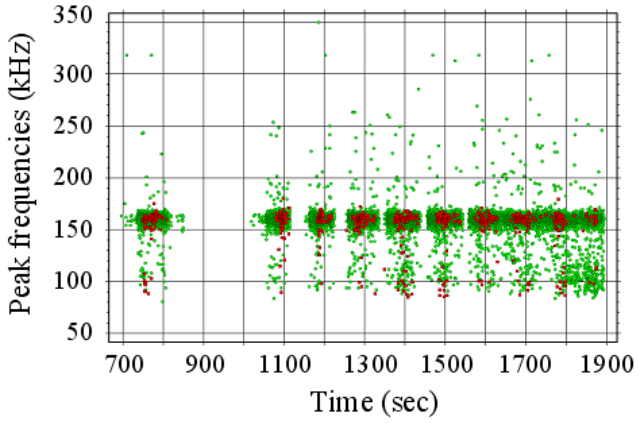

(a) 0% corrosion level

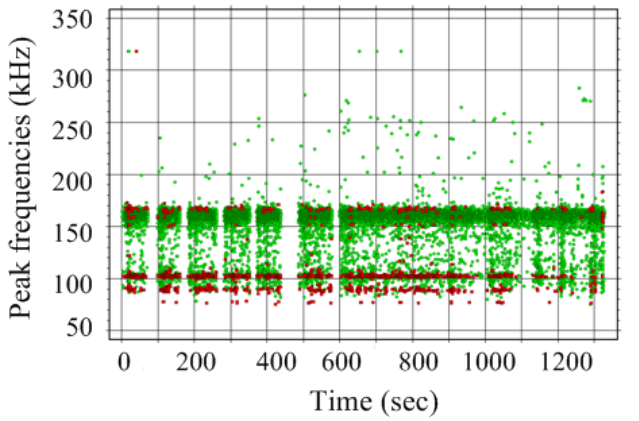

(b) 30% corrosion level

Figure 11. Raw data of peak frequency through FFT.

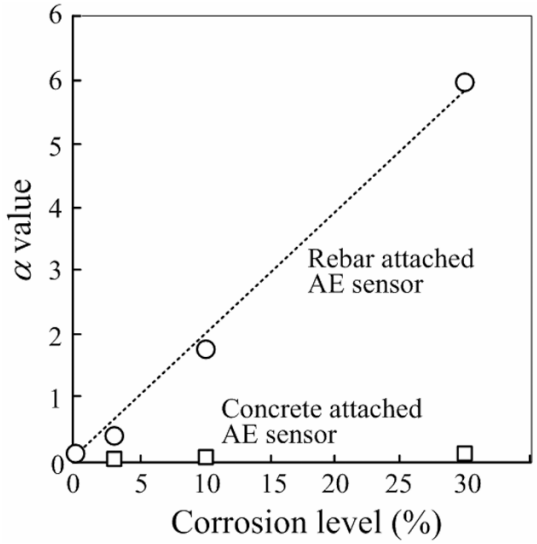

Figure 12. α -value with corrosion levels.

in Figures 11a and b, respectively. No remarkable trends of peak frequencies in every AE hit correlating to corrosion levels could not be confirmed for the concrete attached AE sensor (see green dots), however, with regard to the rebar attached sensor (see red dots) obvious majority shift of the peak frequency from more than 150 kHz to about 100 kHz was obtained. Specifically the upper and lower ranges of the shift, showing those of distribution of AE hits in peak frequencies, can be drawn as 150-180 kHz and 80-110 kHz, respectively. In addition, the shift appeared to be proportional to the corrosion level, α-value is defined as in the following Equation (1),

$$\alpha = \frac{CAH_{low}}{CAH_{high}} \quad (1)$$

where CAE_{low} is cumulative AE hits having peak frequency between 80-110 kHz, and CAE_{high} is cumulative AE hits having peak frequency between 150-180 kHz.

α for the case of rebar attached AE sensor as well as of concrete can be found as in Figure 12. There is no interesting trend between α and corrosion level for the case of concrete, whereas surprisingly linear regression was possible for the case of rebar attached sensor, suggesting that the corrosion level could be assessed by the α-value.

4 CONCLUSIONS

Flexural failure tests of RC beams with different corrosion levels were carried out with monitoring acoustic emissions. Attaching the sensors onto the concrete surface as well as rebar edge faces, AE activity were examined to extract characteristic AE features corresponding to the corrosion level. Through the experimental work, it was clarified that the number of AE events of high frequency dramatically decrease with progress of corrosion in comparison to those of low frequency when using the AE activity of rebar attached sensors. The ratio of AE events of low frequency to those of high frequency, which is defined as α-value, yields to provide the corrosion level quantitatively.

REFERENCES

Ohtsu, M., Tomoda, Y., Sakata, Y., Murata, M. & Matsushita, H. 2003. In-situ monitoring and diagnosis of RC members in an exposure test against salt attack, Proceedings of the 10th International Conference on Structural Faults and Repair. (CD-ROM)

Ohtsu, M. & Tomoda, Y. 2008. Phenomenological model of corrosion process in reinforced concrete identified by acoustic emission, ACI Materials Journal, No.105-M23: 194-199.

Shiotani, T. & Ohtsu, M. 1999. Prediction of slope failure based on AE activity, Acoustic Emission: Standards and Technology Update, ASTM STP 1353, S. J. Vahaviolos, Ed., ASTM: 156-172.

Tamori, K., Maruyama, M., Odagawa, M. & Hashimoto, C. 1988. Crack behavior of reinforce concrete members due to corrosion of reinforcing bar, Proceeding of the Japan Concrete Institute, 10(2): 505-510. (in Japanese)

Yoo, D.J., Weiss, W.J. & Shah, S.P. 2000. Assessing damage in engineering mechanics, ASCE, V. 126, No. 3:273-283.